Volume 58(4): 345–358, 2010
Journal of Histochemistry & Cytochemistry
http://www.jhc.org

ARTICLE

Synthesis and Organization of Hyaluronan and Versican by Embryonic Stem Cells Undergoing Embryoid Body Differentiation

Shreya Shukla,[1] Rekha Nair,[1] Marsha W. Rolle, Kathleen R. Braun, Christina K. Chan, Pamela Y. Johnson, Thomas N. Wight, and Todd C. McDevitt

Wallace H. Coulter Department of Biomedical Engineering, Georgia Institute of Technology and Emory University, Atlanta, Georgia (SS,RN,TCM); Benaroya Research Institute at Virginia Mason, Seattle, Washington (MWR,KRB,CKC,PYJ,TNW); Department of Biomedical Engineering, Worcester Polytechnic Institute, Worcester, Massachusetts (MWR); and Parker H. Petit Institute for Bioengineering and Bioscience, Georgia Institute of Technology, Atlanta, Georgia (TCM)

SUMMARY Embryonic stem cells (ESCs) provide a convenient model to probe the molecular and cellular dynamics of developmental cell morphogenesis. ESC differentiation in vitro via embryoid bodies (EBs) recapitulates many aspects of early stages of development, including the epithelial–mesenchymal transition (EMT) of pluripotent cells into more differentiated progeny. Hyaluronan and versican are important extracellular mediators of EMT processes, yet the temporal expression and spatial distribution of these extracellular matrix (ECM) molecules during EB differentiation remains undefined. Thus, the objective of this study was to evaluate the synthesis and organization of hyaluronan and versican by using murine ESCs during EB differentiation. Hyaluronan and versican (V0 and V1 isoforms), visualized by immunohistochemistry and evaluated biochemically, accumulated within EBs during the course of differentiation. Interestingly, increasing amounts of a 70-kDa proteolytic fragment of versican were also detected over time, along with ADAMTS-1 and -5 protein expression. ESCs expressed each of the hyaluronan synthases (HAS) -1, -2, and -3 and versican splice variants (V0, V1, V2, and V3) throughout EB differentiation, but HAS-2, V0, and V1 were expressed at significantly increased levels at each time point examined. Hyaluronan and versican exhibited overlapping expression patterns within EBs in regions of low cell density, and versican expression was excluded from clusters of epithelial (cytokeratin-positive) cells but was enriched within the vicinity of mesenchymal (N-cadherin-positive) cells. These results indicate that hyaluronan and versican synthesized by ESCs within EB microenvironments are associated with EMT processes and furthermore suggest that endogenously produced ECM molecules play a role in ESC differentiation. This manuscript contains online supplemental material at http://www.jhc.org. Please visit this article online to view these materials. **(J Histochem Cytochem 58:345–358, 2010)**

KEY WORDS
embryonic stem cells
embryoid body
hyaluronan
versican
epithelial–mesenchymal transition
extracellular matrix

PLURIPOTENT EMBRYONIC STEM CELLS (ESCs), derived from the inner cell mass of preimplantation blastocysts, have the ability to differentiate into all somatic cell types, as well as germ cells (Evans and Kaufman 1981; Martin 1981; Wobus et al. 1984; Thomson et al. 1998). Differentiation of ESCs into ectoderm, mesoderm, and endoderm derivatives can be induced in vitro via the aggregation of cells into three-dimensional clusters referred to as embryoid bodies (EBs), which serve as a model of peri-implantation development (Doetschman et al. 1985; Itskovitz-Eldor et al. 2000). For nearly 30 years, murine ESCs have provided an accessible in vitro model system for studying various aspects of early mammalian embryonic morphogenesis (Gossler

Correspondence to: Todd C. McDevitt, PhD, 313 Ferst Drive, Suite 2102 Atlanta, GA 30332-0535. E-mail: todd.mcdevitt@bme.gatech.edu

[1]These authors contributed equally to this work.

Received for publication August 11, 2009; accepted December 9, 2009 [DOI: 10.1369/jhc.2009.954826].

et al. 1989; Robbins et al. 1990), including the differentiation of ESCs into distinct functional cell types, such as cardiomyocytes, neurons, and endocrine cells (among many others) (Robbins et al. 1990; Bain et al. 1995; D'Amour et al. 2006). Although genetic and phenotypic changes of differentiating ESCs have been the primary focus of most studies, the associated dynamic changes in endogenous extracellular matrix (ECM) synthesis and organization that occur coincidentally with differentiation have not been examined as rigorously.

During early development, the epithelial–mesenchymal transition (EMT) is a critical process in embryogenesis whereby epithelial progenitor cells transform into mesenchymal cells to migrate and facilitate tissue formation. This transition is typically characterized by a decreased expression of adherens junctions responsible for coupling the cells tightly together, thereby permitting an increase in cell motility. In an effort to further define the potential for using ESCs as an in vitro model of early development, researchers have studied the EMT in ESCs of mouse (Spencer et al. 2007), rhesus monkey (Behr et al. 2005; Denker et al. 2007), and human (D'Amour et al. 2005; Eastham et al. 2007; Ullmann et al. 2007). ESCs that were differentiated using various strategies ranging from feeder-free conditions (Ullmann et al. 2007), definitive endoderm formation (D'Amour et al. 2005), monolayer (Eastham et al. 2007), and spontaneous differentiation (Spencer et al. 2007) have been shown to mimic aspects of EMT events, evidenced in part by the loss of E-cadherin and the tight junction-associated proteins, as well as increased expression of N-cadherin and mesenchymal transcription factors. In addition to the differential expression of these cell junction markers and transcription factors, cell differentiation and tissue formation in the developing embryo are accompanied by spatially distinct alterations in the composition of the ECM (Wan et al. 1984; Ffrench-Constant and Hynes 1989; Fenderson et al. 1993). However, specific ECM molecules associated with EMT processes in ESCs have yet to be defined.

ECM molecules such as hyaluronan and versican are critically important in regulating EMT processes in various tissues (Henderson and Copp 1998; Mjaatvedt et al. 1998; Camenisch et al. 2000; Zoltan-Jones et al. 2003; Toole et al. 2005; Kern et al. 2006). Hyaluronan is a high-molecular mass (10^6–10^7 Da) glycosaminoglycan (GAG) composed of repeating disaccharide units of glucuronic acid and N-acetylglucosamine that can be synthesized by three independent hyaluronan synthases (HAS), HAS-1, -2, and -3 (Toole 2004). Hyaluronan has been implicated in several morphogenic cell and tissue events involving EMTs, including embryonic development, wound healing, and angiogenesis (West et al. 1985; Foschi et al. 1990; Trabucchi et al. 2002; Schoenfelder and Einspanier 2003; Allison and Grande-Allen 2006). Versican is a chondroitin sulfate proteoglycan found in a variety of soft tissues and is capable of binding to hyaluronan (Wight 2002). Four different isoforms of versican (V0, V1, V2, and V3) exist as a result of alternative splicing of the two exons that encode the GAG attachment domains (α-GAG and β-GAG) in the core protein. Versican affects cell phenotypes associated with EMT processes, including proliferation and migration (Wight 2002), suggesting that hyaluronan and versican together may play functional roles in EMTs occurring during embryonic development.

The objective of this study was to examine the temporal and spatial patterns of hyaluronan and versican expression, accumulation, and organization by mouse ESCs (mESCs) undergoing EB differentiation. The presence and spatial distribution of hyaluronan and versican within differentiating EBs was examined histologically, and hyaluronan and versican extracted from EBs were quantified as a function of differentiation time. The temporal gene expression profile of the individual *HAS* and *versican* isoforms was assessed over the course of early differentiation. In addition, the presence of primitive epithelial and mesenchymal cell populations was assessed relative to the spatial distribution of versican and hyaluronan within the ECM of EBs. These studies demonstrate that dynamic changes in hyaluronan and versican occur coincidentally with phenotypic changes observed during EB differentiation, indicative of EMT processes.

Materials and Methods

Cell Culture

mESCs [D3 cell line (ATCC; Manassas, VA)] were cultured on 0.1% gelatin-coated 100-mm polystyrene cell culture dishes (Corning; Corning, NY) with DMEM (Mediatech; Herndon, VA) supplemented with 15% FBS (HyClone; Logan, UT), 2 mM L-glutamine (Mediatech), 1× MEM nonessential amino acids (Mediatech), antibiotic/antimycotic agents (Mediatech), and 0.1 mM β-mercaptoethanol (MP Biomedicals, LLC; Solon, OH). To maintain the undifferentiated cells, 10^3 U/ml leukemia inhibitory factor (LIF) (ESGRO; Temecula, CA) was added to the culture medium, and cells were passaged every 2 to 3 days before reaching >70% confluence. All of the described studies were performed with ESCs between passages 18 and 30. To initiate EB cultures, a single cell suspension of 4×10^5 ESCs/ml (in 10 ml) was added to 100-mm bacteriological grade Petri dishes (Corning) in culture medium lacking LIF (differentiation medium). Cultures were placed on rotary orbital shakers (model 2314; Barnstead Lab-Line, Dubuque, IA) at 40 rpm at 37C in 5% CO_2 for the entire duration of suspension culture, similar to previously described methods (Carpenedo et al. 2007).

EBs were re-fed every other day after EBs were collected via gravity-induced sedimentation in conical tubes and re-suspended in fresh differentiation medium for additional culture.

Histological Analysis of Hyaluronan and Versican

EBs collected at different stages of differentiation (4, 7, or 10 days) were fixed with 10% formalin for 30 min and embedded in aqueous gel (Histogel; Richard-Allan Scientific, Kalamazoo, MI). Each gel block was processed for histological sectioning through a series of xylene and alcohol rinses prior to being embedded in paraffin. Sections of EB samples (5 μm each) were obtained from different depths (a minimum of 90 μm apart) within the paraffin block and stained with hematoxylin and eosin (H and E) using a Leica AutoStainer XL (Wetzlar, Germany). ESCs fixed with formalin on tissue culture plates were similarly stained with H and E, using the same reagents and incubation times as applied by the autostainer protocol. A minimum of three independent experiments, each containing roughly 3000 EBs, were examined by histological analyses. Paraffin-embedded EBs were also stained using Movat's pentachrome staining procedure after deparaffinization and hydration with distilled water. Sections were incubated in reagents with intermittent rinses performed under running water or ultrapure water, as follows: 1% Alcian blue (20 min), alkaline alcohol (60C, 10 min), Weigert's stain (60 min), Croceine scarlet/acid fuchsin (1 min), 5% phosphotungstic acid (5 min), 1% acetic acid (5 min), 95% ethanol [(EtOH) 1 min], 100% EtOH (2×; 1 min), alcoholic saffron (7 min), and absolute EtOH (2×; 1 min). Slides were then cleared in xylene and mounted with coverslips, using Mount Quick mounting medium (Daido Sangyo Co., Ltd.; Tokyo, Japan).

For immunohistochemical staining, endogenous peroxidase activity was quenched using 0.75% hydrogen peroxide in 100% methanol (20 min), after which the samples were hydrated in a graded ethanol series (100% EtOH–35% EtOH) and rinsed in PBS (pH 7.3). Slides from each block were then incubated in hyaluronidase reaction buffer [50 mM NaOAc, 150 mM NaCl (pH 6.0)] for 1 hour at 37C, with or without hyaluronidase (hyaluronan lyase from *Streptomyces hyalurolyticus*; Sigma, St. Louis, MO), which was diluted to 20 U/ml in hyaluronidase buffer and added to negative control samples. Samples were then blocked in 1% BSA in PBS for 30 min before biotinylated hyaluronan binding protein [HABR-B (2.5 μg/ml); Sigma] was added and incubated overnight at 4C. A Vector Elite ABC kit with Vector Red substrate (both from Vector Laboratories; Burlingame, CA) was used to develop color, and the slides were counterstained with hematoxylin and mounted with coverslips.

For versican staining, sections were deparaffinized, rehydrated, and quenched as described above; treated for 1 hr at 37C with ABCase [chondroitin ABC lyase (MP Biomedicals); 0.2 U/ml in enriched Tris buffer stock, at final concentrations of 50 mM Tris, 60 mM NaAc, 50 mM NaCl (pH 8), with 0.1 mg/ml BSA] as an antigen retrieval step to degrade chondroitin sulfate GAGs and expose the versican core protein. Slides were rinsed in TBS and then blocked for 1 hr at room temperature in 5% Carnation nonfat dry milk. Primary antibody [rabbit anti-mouse versican β-GAG domain (Millipore; Billerica, MA); 7 μg/ml in 0.1% BSA in PBS] was added and incubated overnight at 4C. After three PBS rinses, a biotinylated goat anti-rabbit secondary antibody (1:400 in 0.1% BSA/PBS; Invitrogen, Carlsbad, CA) was added for 1 hr at room temperature. Samples were developed with a Vector Elite ABC kit with Vector Red substrate, and slides were counterstained with hematoxylin and mounted with coverslips. Negative control samples were prepared identically, with rabbit IgG isotype control (7 μg/ml in 0.1% BSA in PBS; Vector Laboratories) used in place of primary antibody.

To visualize hyaluronan and versican in the same section for localization studies, an immunofluorescence (IF) assay was performed. Deparaffinized histological sections were blocked for 1 hr using 1.5% normal donkey serum (NDS). Samples were incubated with the primary reagents HABR-B (2.5 μg/ml; Sigma) and versican (5 μg/ml β-GAG domain; Millipore) together for 1 hr at room temperature or overnight at 4C. After three PBS rinses, the samples were incubated with Alexa 488-streptavidin (Invitrogen; 1:400 in 1.5% NDS; hyaluronan) and tetramethylrhodamine isothiocyanate (TRITC)-labeled donkey anti-rabbit secondary antibody (Jackson ImmunoResearch, West Grove, PA; 1:400 in NDS; versican) for 1 hr at room temperature prior to Hoechst (10 μg/ml) counterstaining. Samples from all stained batches were then mounted with coverslips, using either low-viscosity mounting medium (immunohistochemical samples; Cytoseal 60; Richard-Allan Scientific) or aqueous mounting medium with antifading agents (IF samples) (Gel/Mount; Biomeda Corp., Foster City, CA). Note that antigen retrieval with ABCase was omitted from these samples; ABCase has hyaluronidase activity, which completely degraded hyaluronan in the samples (data not shown). Hyaluronidase treatment and incubation with rabbit IgG isotype in place of primary antibody served as negative controls for hyaluronan and versican staining, respectively.

Immunohistochemical Analysis of ADAMTS-5, Pan-cytokeratin, and N-Cadherin

For ADAMTS-5 staining, deparaffinized histological sections were blocked for 1 hr at room temperature,

using a 2.5% NDS-2.5% BSA solution in PBS. Samples were incubated with rabbit anti-ADAMTS-5 (JSCKNG, 4 μg/ml in 0.1% BSA-PBS; Affinity BioReagents, Rockford, IL) overnight at 4C (negative IgG control: 4 μg/ml in 0.1% BSA-PBS). After three PBS rinses, the samples were incubated with Alexa Fluor 555 (5 μg/ml in 0.1% BSA-PBS) for 1 hr at room temperature prior to Hoechst (10 μg/ml) counterstaining. Samples were then mounted with coverslips using aqueous mounting medium with antifading agents (Gel/Mount).

For pan-cytokeratin and N-cadherin staining, the required antigen retrieval treatments damaged the versican epitope so that colocalization staining could not be performed. Therefore, adjacent sections of each sample were stained for versican as described above. For pan-cytokeratin, antigen retrieval was performed by incubating sections in 40 μg/ml proteinase-K (Fisher Scientific; Pittsburgh, PA) in 10 mM Tris-HCl, pH 8.0 (6 min, room temperature). Samples were then blocked for 1 hr at room temperature in 2% normal goat serum (NGS), followed by incubation with primary antibody recognizing pan-cytokeratin (Dako, Carpinteria, CA; 1:10 dilution in 2% NGS; skin-positive control) overnight at 4C. For N-cadherin staining, heat-induced epitope retrieval was performed by boiling the samples in 10 mM citrate buffer at pH 6.0 for 20 min. Samples were blocked for 1 hr at room temperature in 2% NGS and then incubated with primary antibody recognizing N-cadherin (BD Biosciences, San Jose, CA; 1:30 dilution in 2% NGS; whole-mouse embryo-positive control) overnight at 4C. Both pan-cytokeratin- and N-cadherin-stained samples were visualized by incubation with FITC-labeled goat anti-mouse secondary antibody (Southern Biotech, Birmingham, AL; 1:100 in 2% NGS) for 1 hr at room temperature prior to Hoechst (10 μg/ml) counterstaining. Samples were then mounted with coverslips by using aqueous mounting medium with antifading agents (IF samples; Gel/Mount; Biomeda Corp.).

Microscopy

Histology sections were imaged using a Nikon 80i microscope and a Spot Flex camera (Diagnostic Instruments, Inc.; Sterling Heights, MI). For each antigen sample examined, images for all samples were acquired using the same exposure settings. Slight linear adjustments in brightness were made across entire images using SPOT advanced software to enhance the contrast between signal and background.

Quantitative Hyaluronan Expression in EBs

Hyaluronan was isolated from ESCs, EBs (50,000 cells per sample; $n = 3$ for each time point), or the medium conditioned by the cells by digestion with Pronase [500 μg/ml; 15 mg/ml stock in 0.5M Tris (pH 6.5); Pronase from *Streptomyces griseus* (Roche Applied Science; Indianapolis, IN)] at 37C overnight. The enzyme was then heat-inactivated at 100C for 20 min, and the samples were stored at −20C prior to analysis. Hyaluronan was quantified using a hyaluronan test kit (Corgenix; Denver, CO) by diluting the samples in 10 volumes of reaction buffer and adding 100 μl to hyaluronic acid binding protein (HABP)-coated microwells (1 hr, room temperature). Wells were then rinsed with PBS, and 100 μl of horseradish peroxidase–conjugated HABP solution was added (30 min, room temperature). Each well was rinsed an additional four times prior to a 30-min incubation (room temperature) with 100 μl of substrate solution (3,3′,5,5′-tetramethylbenzidine and hydrogen peroxide). Blue color developed in positive samples, and 100 μl of stopping solution (0.36 N sulfuric acid) was added to each well. The optical density for each well was read at 450 nm with a spectrophotometer (SpectraMax M2e model; Molecular Devices, Sunnyvale, CA). A standard curve created from purified hyaluronan was used to calculate hyaluronan concentration in cell samples, which are presented normalized to cell number. Cell number was determined by dissociating EBs and counting individual cells with a hemacytometer.

Western Blotting

Protein was isolated from ESCs and day-4, -7, and -10 EBs with extraction buffer [8 M urea, 2 mM EDTA, 50 mM Tris, 0.5% Triton X-100, 0.25 M NaCl, protease inhibitor cocktail (Roche)]. Protein concentrations were measured using a MicroBCA assay (Pierce; Rockford, IL), and samples were stored at −80C prior to analysis. For versican blots, 300 μg of total protein per sample was applied to diethylaminoethyl (Sephacel; Sigma) columns (0.3-ml bed volume), preequilibrated, and washed with 10 bed volumes of wash buffer (8 M urea, 2 mM EDTA, 50 mM Tris, 0.5% Triton X-100, 0.25 M NaCl). The samples were eluted with 3 bed volumes of wash buffer containing 2 M NaCl. Chondroitin sulfate [50 μg/ml; 10 mg/ml stock (Sigma)] carrier was added, and protein was precipitated from the eluate by adding ethanol (95% ethanol-1.3% potassium acetate) for 2 hr at −80C. Precipitated protein was collected by centrifugation for 5 min at 14,000 rpm and rinsed twice with ethanol. Pellets were air dried and then digested with 3 U/ml chondroitinase (10 U/ml stock; Seikagaku, Tokyo, Japan) in 20 mM Tris, 3.6 mM sodium acetate (pH 8.0) for 3 hr at 37C to remove chondroitin chains from the core proteins. Concentrated sample buffer [50 mM Tris-HCl (pH 6.8), 1% SDS, 10% glycerol, 1.7% (v/v) 2-mercaptoethanol] was added, and the samples were boiled for 3 to 4 min prior to being loaded onto a 15-cm × 12-cm 4% to 12% gradient polyacrylamide gel (3.5% stacking gel) and separated overnight at room temperature. Protein was

transferred to nitrocellulose membranes and blocked for 2 hr at room temperature in blocking buffer (2% BSA in Tris-buffered saline, 0.1% Tween-20). Membranes were incubated overnight in blocking buffer containing 2% calf serum and 0.25 μg/ml rabbit anti-mouse versican β-GAG domain antibody (Millipore). Membranes were then washed with TBS-T (Tris-buffered saline with 0.1% Tween-20) and incubated for 2 hr at room temperature [1:20,000 goat anti-rabbit IgG antibody conjugated to alkaline phosphatase in blocking buffer (Jackson ImmunoResearch)]. After blots were extensively washed in TBS-T, they were incubated in assay buffer [0.1 M diethanolamine, 1 mM $MgCl_2$, 0.02% sodium azide (pH 10)] for 10 min, followed by incubation with substrate (1:100 CSPD chemiluminescent substrate, 1:20 Nitro-Block membrane enhancer in assay buffer; Applied Biosystems, Foster City, CA) for 5 min at room temperature. Blots were exposed to autoradiograph film (ISC BioExpress; Kaysville, UT) and developed in a film processor (Fischer Industries Inc.; Geneva, IL). For DPEAAE blots, equal amounts of protein from each sample were ethanol precipitated and electrophoresed on 8% SDS-PAGE with 3.5% stacking gel. Proteins were transferred to nitrocellulose, probed with DPEAAE antibody (1 μg/ml; Affinity Bioreagents, Golden, CO), and detected using an enhanced chemiluminescence kit as described above. As a loading control, the same blot was also probed with an anti-actin N-terminal antibody (Sigma).

Each lane on the Western blots shown represents protein lysates from an EB culture collected at the designated time point. Lysates from three separate cultures per time point were examined for each independent experiment.

Quantitative RT-PCR (qRT-PCR)

RNA was extracted from undifferentiated ESCs and EBs at days 4, 7, and 10 of differentiation using an RNeasy mini-kit (Qiagen; Valencia, CA). Complimentary DNA was reverse transcribed from 1 μg of total RNA, using an iScript cDNA synthesis kit (Bio-Rad; Hercules, CA), and real-time RT-PCR was performed using SYBR Green technology with a MyiQ cycler (Bio-Rad). Beacon designer software was used to design forward and reverse primers (Invitrogen) (see Supplemental Table ST1) for the pluripotency markers *Oct-4* and *Nanog*, the three HAS isoforms (*HAS-1*, *HAS-2*, and *HAS-3*), the four versican splice variants (*V0*, *V1*, *V2*, and *V3*), and glyceraldehyde-3-phosphate dehydrogenase (*GAPDH*), which were then validated with the appropriate positive controls. Gene expression of *Oct-4* and *Nanog* was calculated relative to undifferentiated ESC samples by using the Pfaffl method (Pfaffl 2001), while HAS and versican concentrations were calculated from standard curves prior to normalization to GAPDH expression levels. Gene expression data from two independent batches of ESCs and EBs each containing three replicates cultured at different times ($n=6$ for each time point) were combined prior to statistical analyses.

For SuperArray RT^2 Profiler PCR array analysis, cDNA synthesis was performed using a SuperArray RT^2 First Strand kit (SABiosciences; Frederick, MD). First, the genomic DNA elimination mixture was prepared by mixing 0.5 μg of RNA with the 5× genomic DNA elimination buffer and RNase-free water and incubated at 42C for 5 min. The RT cocktail (5× RT buffer 3, primer and external control mixture, RT enzyme mixture 3, and RNase-free water) was prepared (10 μl) and added to the elimination buffer mixture. Each sample was then placed in an iCycler thermal cycler (Bio-Rad) for synthesis (15 min at 42C, 5 min at 95C) and diluted with RNase-free water. RT-PCR was performed by first preparing the experimental cocktail (1275 μl of 2× SuperArray RT^2 qPCR Master Mix, 102 μl of diluted first-strand cDNA synthesis reaction, 1173 μl of RNase-free water) and then distributing it across all wells of the PCR 96-well array. The array was tightly sealed with optical thin-wall 8-cap strips and run in a MyiQ cycler (Bio-Rad) with a two-step cycling program (1 cycle of 10 min at 95C; 40 cycles of 15 sec at 95C; and 40 cycles of 1 min at 60C) and melt curve. Fold changes in gene expression were analyzed using the threshold cycle ($\Delta\Delta C_t$) method of quantitation, whereby samples of EBs from different time points (days 4, 7, and 10) were compared to undifferentiated ESC values after individual sample values were normalized to GAPDH levels.

Statistics

For paired comparisons, Student *t* tests assuming unequal variances were used to determine statistical significance ($p<0.05$). For comparisons across multiple groups, ANOVA was performed using a 95% confidence interval followed by post hoc Tukey analysis to determine significant differences ($p<0.05$) between the different experimental groups.

Results

Embryoid Body Differentiation

Adherent colonies of undifferentiated mESCs were dissociated into single cells and reaggregated in suspension culture to form cell spheroids constituting putative EBs (see Supplemental Figure SF1). As expected, the resulting EBs increased in size and adopted a more differentiated morphology over the course of differentiation, indicated by the formation of a primitive endoderm layer on the periphery of EBs (shown by solid arrows in Supplemental Figure SF1), as well as cystic cavities (hollow arrows, Supplemental Figure SF1) that developed in the interior of the EBs. Phenotypic differentiation

of the EBs was evident as a reduction in the expression of the *Oct-4* and *Nanog* pluripotent transcription factors by EBs over time (see Supplemental Figure SF2), as well as a coincident decrease in *E*-cadherin and an increase in *N*-cadherin gene expression (see Supplemental Figure SF3). Progressive differentiation was also indicated by the acquisition of more mature phenotypic markers, such as α-*fetoprotein*, *GATA-4*, *nestin*, *Nkx 2.5*, and α-*myosin heavy chain* (data not shown). Movat's pentachrome staining of EBs revealed intense cytoplasmic staining (red) of densely packed epithelium-looking cells at early stages of differentiation (days 4 and 7). After 10 days, a majority of cells within many EBs adopted a more mesenchymal appearance, and GAGs were detected in the extracellular space (light blue) throughout EBs (see Supplemental Figure SF4), which appeared to be the primary ECM component synthesized at the times examined.

Hyaluronan and Versican Accumulation and Distribution Within Differentiating EBs

To specifically examine the spatial distribution of hyaluronan and versican within EBs, immunohistochemistry was performed to examine EBs at different stages of differentiation (days 4, 7, and 10). After only 4 days of differentiation, very little hyaluronan was detected in EBs (Figures 1A, 1D, and 1G), but that which was present was predominantly localized around the periphery of most of the cell aggregates. By differentiation day 7, hyaluronan was clearly detectable more extensively throughout EBs and most often appeared to be enriched primarily on one side of an EB (Figures 1B, 1E, and 1H). After day 10, hyaluronan was found to be distributed throughout almost the entire interior of EBs (Figures 1C, 1F, and 1I). Interestingly, the accumulation of hyaluronan appeared to be greatest in areas of lower cell density within EBs. Similarly, versican (detected with an antibody recognizing the V0/V1 isoforms of versican) was minimally present within EBs at day 4 of differentiation (Figures 2A, 2D, and 2G) but was distributed throughout a large portion of EBs by day 7 of differentiation (Figures 2B, 2E, and 2H). After 10 days of differentiation, versican was detected throughout the majority of EBs and appeared most concentrated within less dense areas of cells (Figures 2C, 2F, and 2I), in patterns similar to those observed for hyaluronan localization. Thus, the expression levels of hyaluronan and

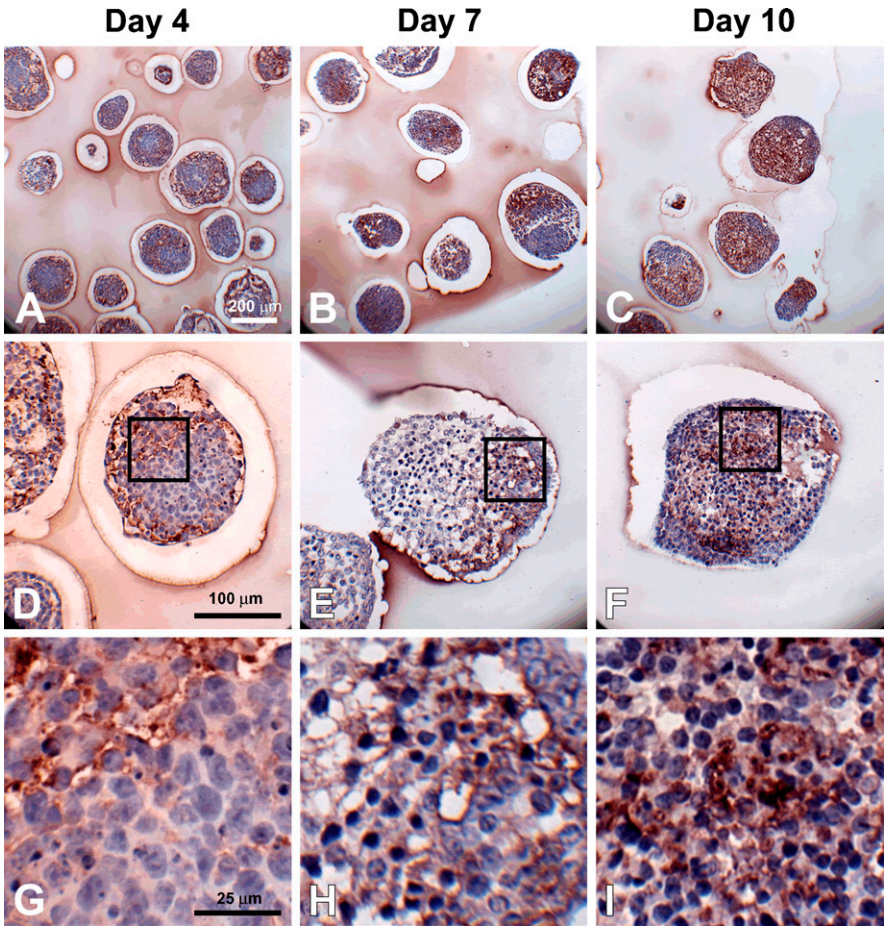

Figure 1 Hyaluronan accumulation during embryoid body (EB) formation. Sections (5 μm) from day 4, 7, and 10 EBs were stained with hyaluronan binding protein (dark red color); hematoxylin-stained nuclei are shown in blue. Hyaluronan was increasingly prominent with differentiation time (**A–C**). Localized pockets of hyaluronan staining can be seen by day 7 (**B,E**), and higher magnification (**G–I**, magnified view of boxes in **D–F**) shows hyaluronan surrounding individual cells. Scale bars at left apply to each row.

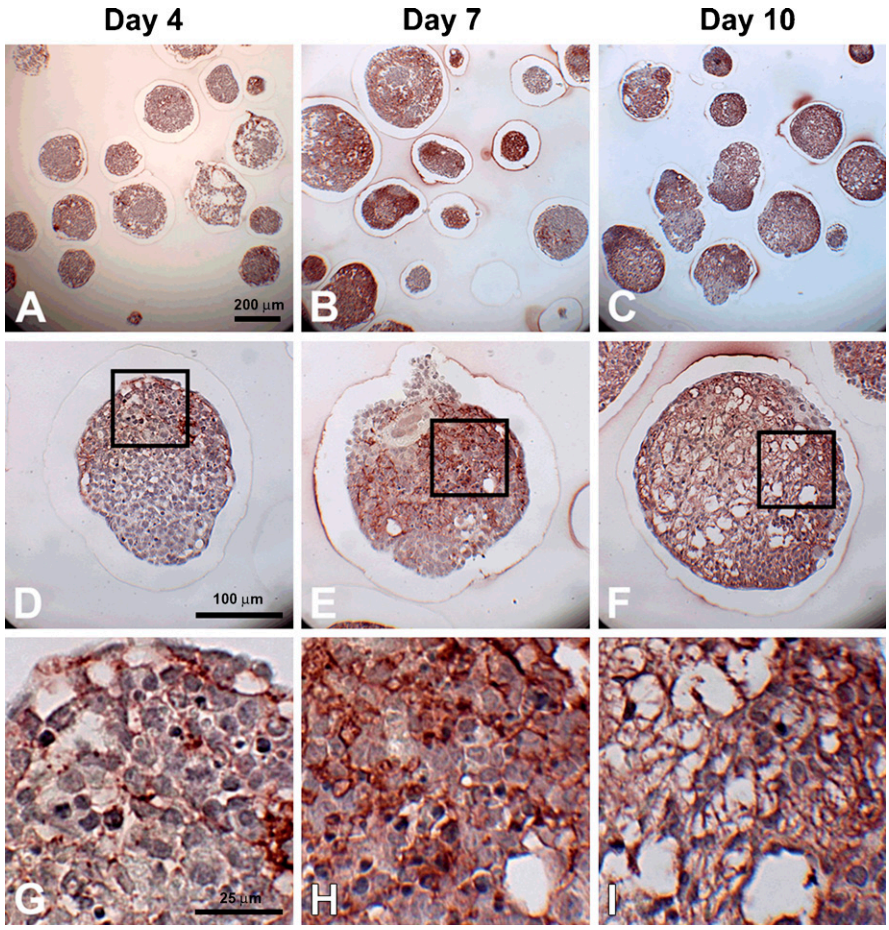

Figure 2 Versican accumulation during EB formation. Sections (5 μm) from day 4, 7, and 10 EBs were stained with anti-versican antibody (dark red color); hematoxylin-stained nuclei are shown in blue. Some versican expression can be seen by day 4 (**A,D**), with increased quantities observed by days 7 (**B,E**) and 10 (**C,F**). Versican (V0 and V1 isoforms) appears to localize in areas of lower cell density, while higher magnification images (**G–I**, magnified view of boxes in **D–F**) reveal versican staining within acellular spaces. Scale bars at left apply to each row.

versican within EBs exhibited similar temporal and spatial patterns over the course of differentiation.

Accumulation of Hyaluronan During EB Formation

To quantify the amount of hyaluronan synthesized and retained within EBs and released into the medium over the course of differentiation, hyaluronan produced by EBs was assessed using a hyaluronan binding protein quantification kit (Figure 3). Hyaluronan accumulated within EBs as a function of time, such that the relative amount of hyaluronan by day 10 of differentiation increased significantly compared with that of earlier time points (ESCs, $p = 0.002$; day 4, $p = 0.003$; day 7, $p = 0.006$). The quantity of hyaluronan produced per cell and retained within day-10 EBs was almost 30-fold greater than the amount of hyaluronan retained in the cell layer by undifferentiated ESCs (range, 0.090 ± 0.07 pg/cell to 2.680 ± 1.11 pg/cell) (Figure 3A). Likewise, the concentration of hyaluronan secreted into the culture medium increased almost four-fold from 0.898 ± 0.13 μg/ml at day 2 to 3.572 ± 0.59 μg/ml by day 10 of EB culture. For the first 6 days of differentiation, ESC- and EB-conditioned media contained similar concentrations of hyaluronan, between 0.898 ± 0.13 μg/ml and 1.594 ± 0.32 μg/ml (Figure 3B). However, hyaluronan content significantly increased at days 8 and 10 of differentiation (2.769 ± 0.42 μg/ml and 3.572 ± 0.59 μg/ml, respectively) compared with the earlier time points examined. When evaluated on a per cell basis, it is clear that the ratio of hyaluronan in the medium compared with hyaluronan retained within the EBs steadily declined over the course of differentiation. Medium conditioned by day 4, 7, and 10 EBs contained 0.354 ± 0.072 pg of hyaluronan/cell, 0.157 ± 0.0058 pg of hyaluronan/cell, and 0.274 ± 0.046 pg of hyaluronan/cell, respectively, compared with 0.167 ± 0.06 pg hyaluronan/cell (day 4), 0.480 ± 0.22 pg hyaluronan/cell (day 7), and 2.68 ± 1.1 pg hyaluronan/cell (day 10) retained within the EBs. Altogether, these results indicate that EBs synthesize and secrete increasing amounts of hyaluronan as a function of differentiation and that an increasing amount of hyaluronan is retained within EBs over time.

Versican Accumulation and Proteolytic Processing During EB Formation

To further analyze versican synthesis and accumulation by differentiating EBs, proteoglycans were isolated and

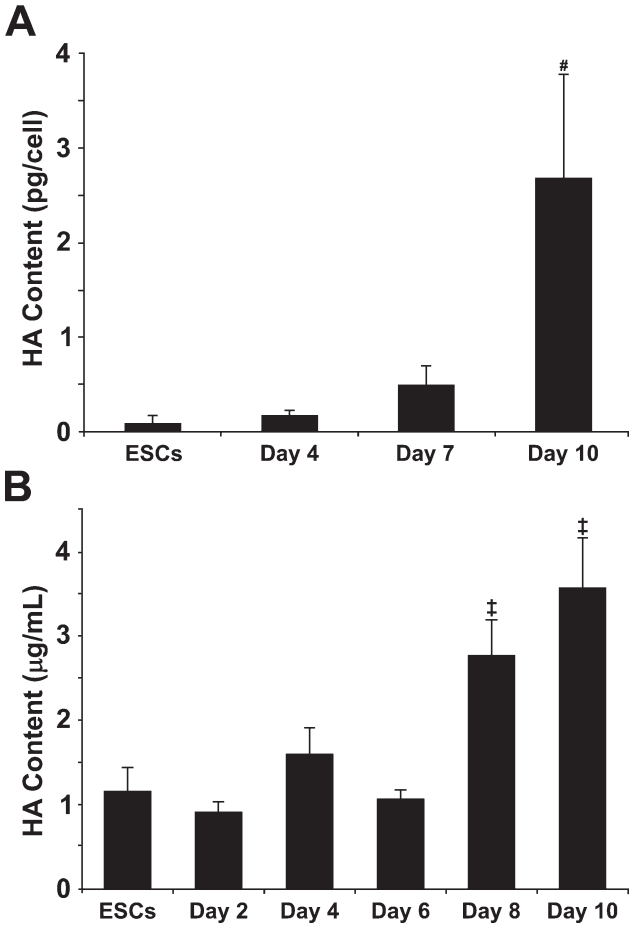

Figure 3 Quantification of hyaluronan synthesis by EBs. A quantitative hyaluronan (HA)-binding protein-based kit was used to measure hyaluronan retained within embryonic stem cells (ESCs) and day 4, 7, and 10 EBs (**A**) as well as hyaluronan secreted in medium conditioned by ESCs and day 2, 4, 6, 8, and 10 EBs (**B**). Hyaluronan content in ESCs, EBs, and conditioned medium samples progressively increased over the course of differentiation. Day 10 EBs and day 8- and 10-conditioned media samples contained significantly greater amounts of hyaluronan than samples collected from all other time points examined. (**A**) # indicates significant differences from ESCs, day 4, and day 7 ($p<0.01$); (**B**) ‡ indicates significant differences from ESCs and days 2–6 ($p<0.01$) (ANOVA with post hoc Tukey test). Error bars represent standard deviations; $n=3$ per group.

examined by Western blot analysis using a primary anti-mouse versican β-GAG domain antibody, which detects only the V0 and V1 versican isoforms. Isoforms V0 and V1 usually appear as two high-molecular-mass products that migrate in the 350- to 450-kDa range on SDS-PAGE (Sandy et al. 2001; Kenagy et al. 2006; Seidelmann et al. 2008). For ESCs or EBs after 4 days of differentiation, little, if any, immunoreactivity appeared in the gels above the 250 molecular weight marker where V0 and V1 usually run (Figure 4A). However, by day 7, there was a distinct increase in the amount of protein recognized by the β-GAG antibody, which was further increased at day 10 (Figure 4A). Several bands also appeared near or below the 250-molecular-weight marker in the 10-day EB cultures, most likely representing degradation products of versican (Sandy et al. 2001; Kenagy et al. 2006; Seidelmann et al. 2008). Therefore, to assess whether versican proteolysis occurred during EB differentiation, immunoblotting was performed using an antibody that specifically recognizes DPEAAE, a cleavage neoepitope of versican generated by specific members of the ADAMTS family of enzymes (Sandy et al. 2001). The neoepitope was not detected in undifferentiated ESCs but appeared at day 4 of differentiation and increased in signal intensity through day 10 (Figure 4B). Similarly, gene expression of *ADAMTS-1* (Sandy et al. 2001) and *ADAMTS-5* (Longpre et al. 2009), two enzymes that are known to cleave versican, increased significantly by 10 days of differentiation compared with ESCs (Figure 4C), particularly for *ADAMTS-5*. In contrast, gene expression of *ADAMTS-8*, which is not known to cleave versican, did not change significantly during EB differentiation. Immunostaining for ADAMTS-*5* indicated minimal expression in day-4 EBs (data not shown), but the protease was distributed throughout different regions of day-7 and day-10 EBs (Figures 4D and 4E). Altogether, these results indicate that increased expression and proteolytic processing of versican occur during EB differentiation.

Hyaluronan Synthase and Versican Gene Expression

The relative expression levels of the different HAS genes remained fairly consistent over the course of early EB differentiation (Figure 5A), with expression of *HAS-2* significantly greater than either *HAS-1* or *HAS-3* at each of the time points examined (undifferentiated ESCs and days 4, 7, and 10 of EB differentiation). In contrast, no significant differences were found between *HAS-1* and *HAS-3* expression at any stage of ESC differentiation. In addition, by 10 days of differentiation, *HAS-2* expression was significantly increased ($p<0.01$) compared with the levels measured at all of the earlier time points of analysis.

Similar to the patterns of HAS expression, the relative expression levels of the different versican isoforms were consistent over time (Figure 5B). Undifferentiated ESCs and differentiating EBs expressed relatively high levels of *V0* and *V1* that were each significantly greater than that of *V2* and *V3* at all of the time points examined ($p\leq0.003$ in all cases), except for day 10, when *V0* and *V3* were not statistically different. The expression levels of *V0*, *V1*, and *V3* increased significantly by day 10 of EB differentiation compared with any of the earlier time points ($p<0.01$). However, the expression of *V2* remained relatively low compared with the other versican isoforms and did not change significantly over the course of EB differentiation.

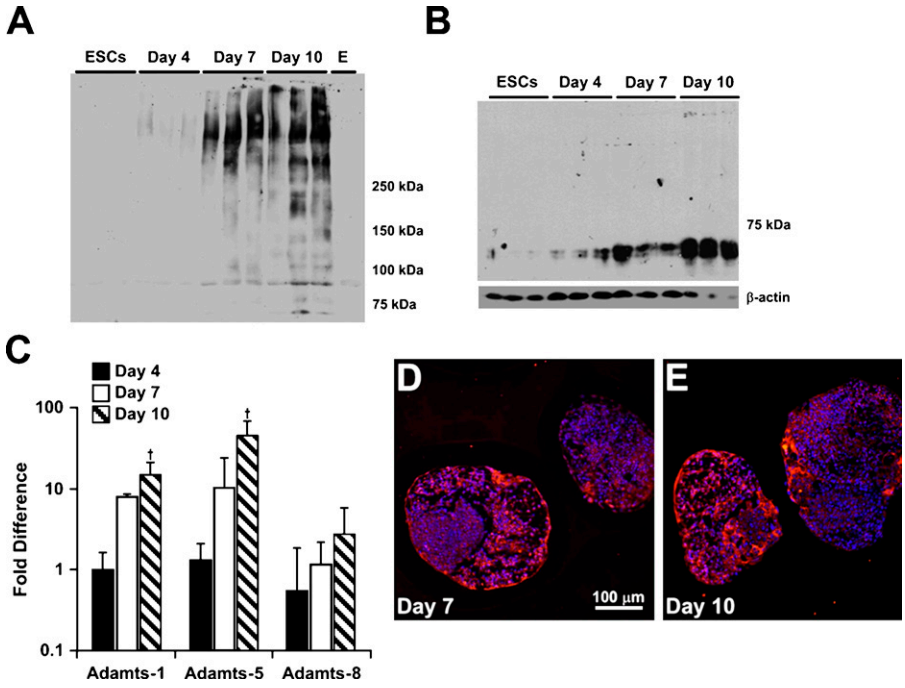

Figure 4 Analysis of versican synthesis and proteolysis in differentiating EBs. Purified, chondroitinase-treated protein lysates from triplicate samples of ESCs and day 4, 7, and 10 EBs were probed with rabbit anti-mouse versican β-GAG domain antibody (**A**). An increase in proteins identified by the β-GAG antibody (versican core proteins V0 and V1, approximately 450 and 350 kDa, respectively) were apparent after 7 and 10 days of differentiation in triplicate samples and were not detected in ESCs and EBs after 4 days of differentiation. Protein lysates were also examined for the versican cleavage product, known as the DPEAAE fragment, generated by ADAMTS-1 over the course of EB culture (**B**). The 70-kDa DPEAAE fragment was present at day 4 and appeared to increase with differentiation time through day 10. β-Actin was used as a loading control. *ADAMTS-1* and *-5*, known versicanases, were examined via SuperArray RT-PCR arrays, and expression of each gene was found to increase significantly by day 10 compared with day 4 of differentiation, while *ADAMTS-8*, a protease unrelated to versican degradation, remained unchanged (**C**). ADAMTS-5 immunofluorescent staining detected protease expression with day 7 (**D**) and day 10 (**E**) EBs. † indicates significant differences from day 4 EBs ($p<0.05$) (ANOVA with post hoc Tukey test). Error bars represent standard deviations; $n=3$ per group.

Hyaluronan and Versican Localization

Immunofluorescent affinity labeling of both hyaluronan and versican within the same sections confirmed that hyaluronan and versican were not detectable in most EBs at 4 days of differentiation, although when present, hyaluronan localized in the same areas as versican (Figures 6A, 6D, 6G, and 6J). By day 7, hyaluronan and versican were distributed in regions of the EBs that primarily contained a lower density of cells (Figures 6B, 6E, 6H, and 6K). The appearance of a largely fibrillar network of overlapping hyaluronan and versican was clearly distinguishable by 10 days of differentiation throughout much of the interior of EBs (Figures 6C, 6F, 6I, and 6L). Thus, at each of the time points examined, hyaluronan and versican were consistently distributed in a similar spatial pattern within differentiating EBs.

Epithelial and Mesenchymal Phenotypes Within EBs

Based on the observed accumulation and overlapping patterns of hyaluronan and versican expression in EBs during differentiation, as well as differences in cell morphology in regions containing hyaluronan and versican, the spatial distribution of epithelial [cytokeratin-positive (cytokeratin+)] and mesenchymal [N-cadherin-positive (N-cadherin+)] cells within EBs were examined relative to versican-rich regions. After 10 days of differentiation, EBs clearly contained distinct populations of cytokeratin+ and N-cadherin+ cells. Cytokeratin+ cells were primarily localized around the periphery of EBs, and versican appeared to be completely excluded from such areas within the same EB (Figures 7A and 7B). In contrast, N-cadherin+ cells were predominantly found within the interior of EBs in regions that overlapped with the presence of versican (Figures 7C and 7D).

Discussion

These studies provide evidence that spatial and temporal patterns of hyaluronan and versican accumulation and organization by ESCs within EBs are associated with epithelial–mesenchymal transitions occurring within the aggregates of differentiating cells. ESCs express several HAS and versican isoforms throughout the course of EB differentiation, concomitant with an increasing accumulation of hyaluronan and versican over the first 10 days of differentiation. The overlapping spatial patterns of expression suggest that hyaluronan and versican are physically associated within EBs and moreover that the overlapping patterns of accumulation of these molecules are found predominantly in regions of EBs containing cells actively undergoing EMT differentiation. Overall, these results not only suggest a specific role for hyaluronan and versican in the morphogenesis of primitive pluripotent stem cells but also demonstrate that dynamic changes in the endogenous expression, accumulation, and processing of

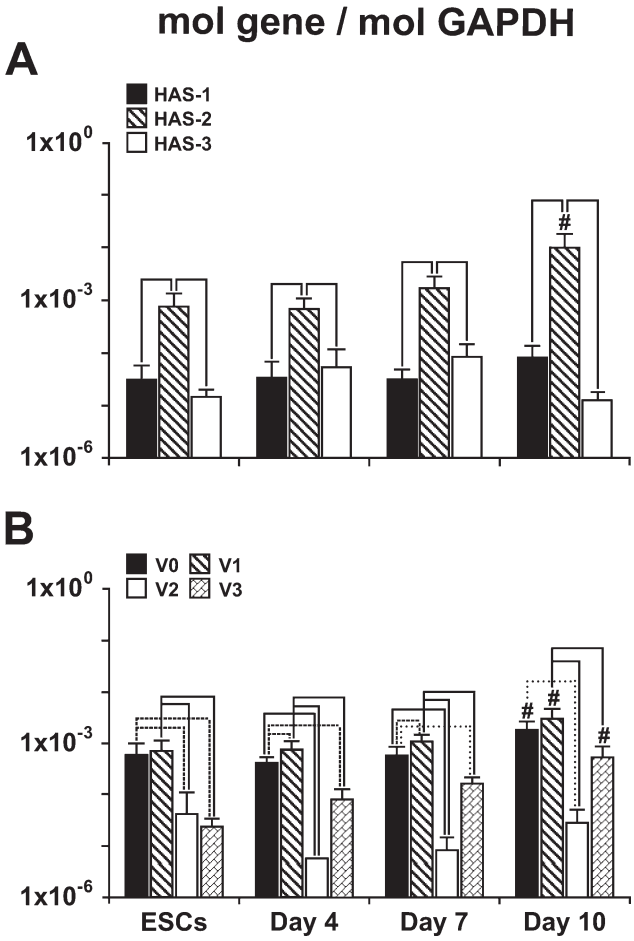

Figure 5 Quantification of hyaluronan synthase (HAS) and versican gene expression. qRT-PCR was used to compare expression levels of HAS isoforms 1, 2, and 3 and versican splice variants V0, V1, V2, and V3 during the course of EB differentiation. *HAS-2* increased with time and was consistently expressed at significantly higher levels than either *HAS-1* or *HAS-3*. Isoforms *V0*, *V1*, and *V3* increased by 10 days of differentiation, while *V2* was consistently expressed at relatively low levels. (**A,B**) # indicates significant differences from ESCs, day 4, and day 7 ($p<0.02$); solid line indicates a p value of <0.01; dashed line indicates $p<0.02$; and dotted line indicates $p<0.05$ (ANOVA with post hoc Tukey test). Error bars represent standard deviations; $n=6$ per group.

ECM molecules by differentiating ESCs occur coincidentally with cell phenotype changes. These results indicate that an improved understanding of the molecular composition of embryonic extracellular matrices could yield new insights into developmental biology and provide novel strategies for the directed differentiation of stem cells.

The most significant and novel finding of the present study is that the timing and spatial distribution of hyaluronan and versican expression within EBs correlate with the appearance and localization of mesenchymal (N-cadherin+) cell phenotypes and is excluded from regions of epithelial (cytokeratin+) cells (Figure 7). Previous studies have demonstrated that ESC differentiation within EBs recapitulates many aspects of gastrulation, including the transformation of epithelial pluripotent cells (resembling primitive ectoderm) into migratory mesenchymal cells (resembling primitive streak) (Behr et al. 2005; D'Amour et al. 2005; Denker et al. 2007; Eastham et al. 2007; Spencer et al. 2007; Ullmann et al. 2007). Thus far, however, dynamic changes in prevalent ECM molecules produced within EBs, such as hyaluronan and versican, have not been directly examined or correlated with distinct populations of cells. It has been previously demonstrated that coincident expression of hyaluronan and versican can stimulate cell migration by creating a viscoelastic, hyaluronan-versican-rich, malleable extracellular environment (Wight 2002; Wight and Merrilees 2004; Allison and Grande-Allen 2006; Ricciardelli et al. 2007). Furthermore, a hyaluronan–versican matrix may influence cell fate by enriching for signaling molecules and growth factors that regulate cell proliferation and differentiation. The importance of hyaluronan and versican in directing EMT processes is clear from a number of examples in cell and developmental biology. Whereas HAS-2$^{-/-}$ mouse embryos fail to undergo EMT during cardiac morphogenesis (Camenisch et al. 2000), overexpression of hyaluronan by HAS-2 recombinant adenoviral infection of normal epithelial cells induces an EMT (Zoltan-Jones et al. 2003). In addition, versican plays an essential role in the EMT of the endocardial mesenchymal cushion (Mjaatvedt et al. 1998; Kern et al. 2006), as well as mesenchymal condensation and hair induction (Kishimoto et al. 1999). Thus, hyaluronan and versican appear to regulate the transformation of epithelial cells to mesenchymal phenotypes at various stages of development.

As noted above, the expression of HAS isoforms, in particular HAS-2, and the synthesis of hyaluronan play important roles in early embryological development of numerous tissues. Although targeted inactivation of both the *HAS-1* and *HAS-3* genes results in viable animals (Spicer et al. 2002), the knock-out of the *HAS-2* gene is embryo lethal by embryo day 9.5 (E9.5). In addition, HAS-2$^{-/-}$ E9.5 embryos almost completely lack

Figure 6 Hyaluronan and versican spatial distributions. EBs were stained for both hyaluronan (green; **A–C**) and versican isoforms V0 and V1 (red; **D–F**); merged images show localization of the two molecules in yellow (**G–I**) and at higher magnifications (**J–L**). Hyaluronan and versican appear to localize in areas of lower cell density, and deposition of both molecules increases over the course of differentiation. Bar in **A** applies to **A–I**; bar in **J** applies to **J–L**.

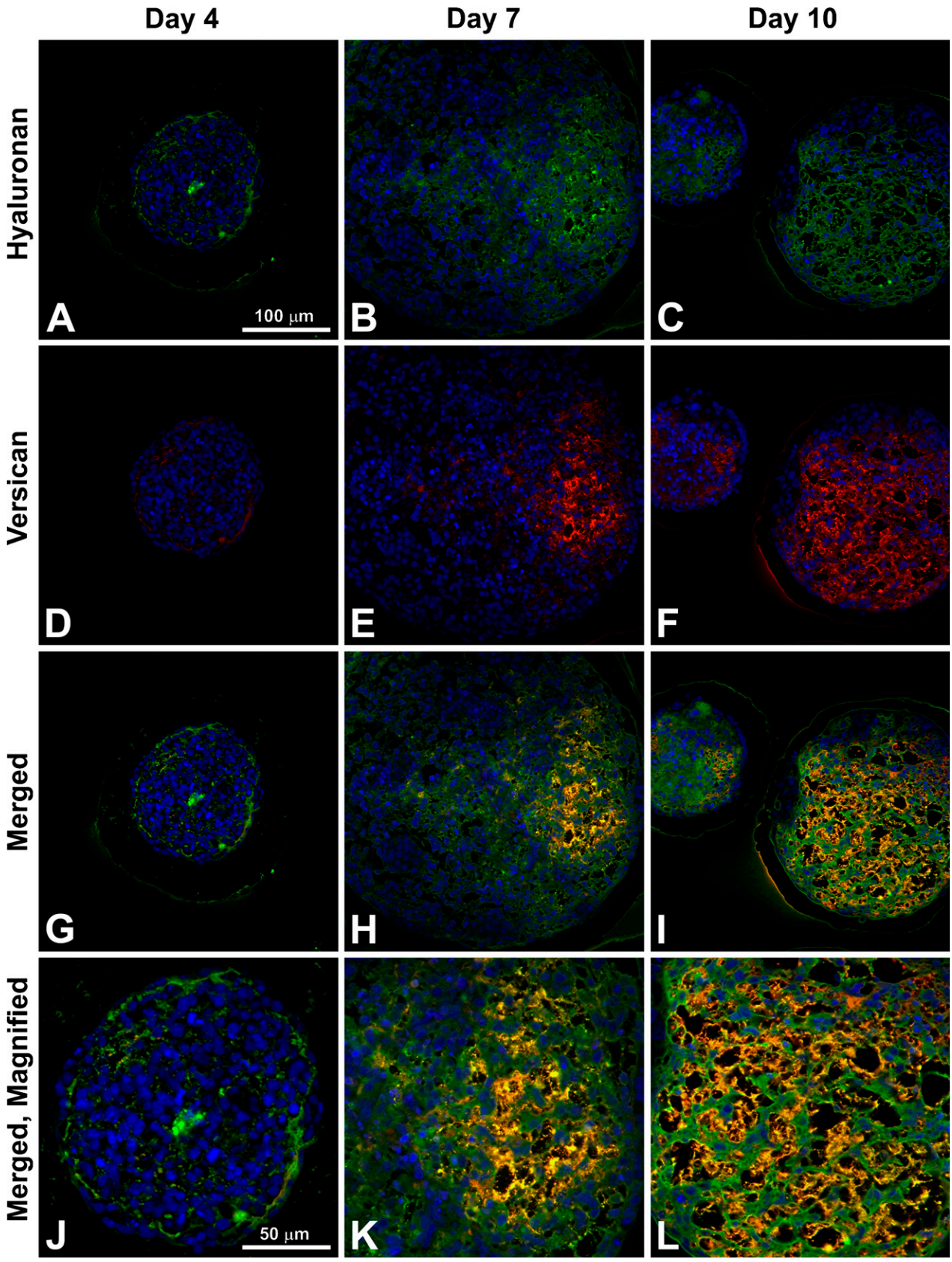

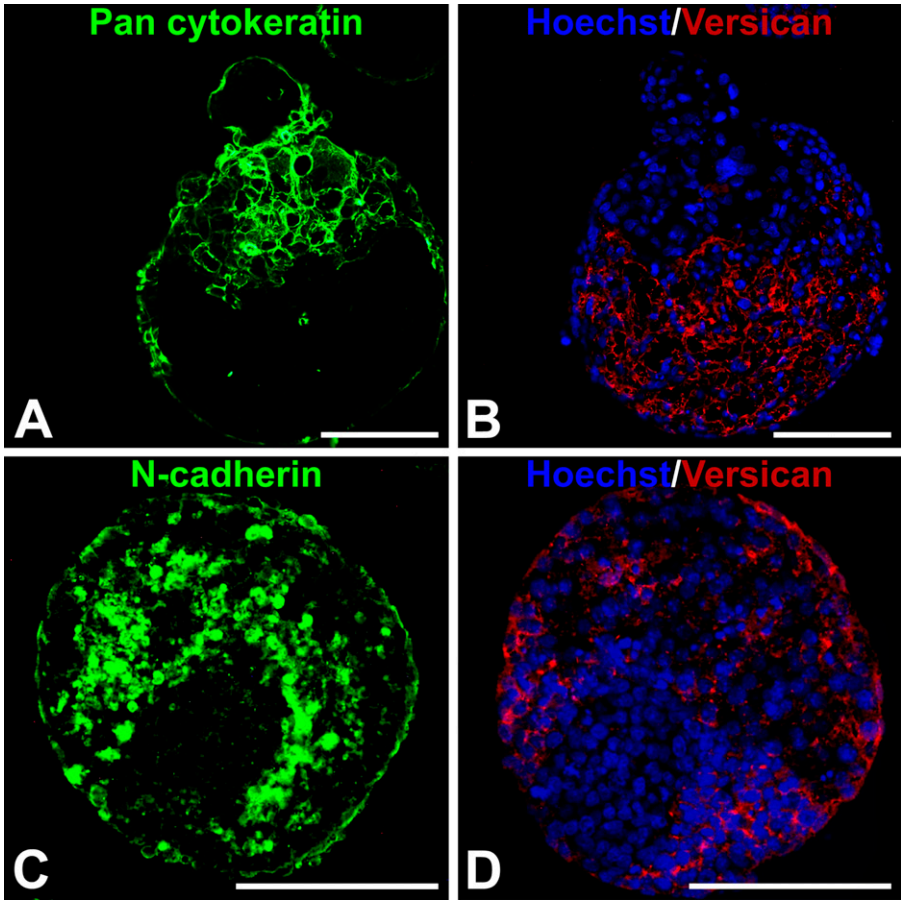

Figure 7 Cellular expression of epithelial–mesenchymal phenotype markers relative to versican localization. Adjacent 5-μm sections from day 10 EBs were fluorescently stained with pan-cytokeratin or N-cadherin primary antibody (FITC-labeled secondary, green) and versican (isoforms V0 and V1; TRITC-conjugated secondary antibody) (red); nuclei were counterstained with Hoechst dye (blue). Cytokeratin localized primarily in the periphery of the EBs, with some evidence of invasion into the EB interiors, while versican was localized exclusively in cytokeratin-negative areas (**A,B**). In contrast, N-cadherin localized to areas occupied by versican (**C,D**). Staining was performed on adjacent sections of the same EBs, which were matched based on morphology and location on each slide. Bar = 100 μm.

hyaluronan, suggesting that HAS-2 is the primary isoform responsible for hyaluronan synthesis during early organogenesis (Camenisch et al. 2000). In the present study, *HAS-2* was the dominant synthase isoform expressed by ESCs in EBs, and *HAS-2* expression increased significantly by 10 days of differentiation. The distribution of hyaluronan within murine EBs increased over time such that after 10 days, differentiating cells produced ~30-fold more hyaluronan than undifferentiated ESCs (Figure 3A). Similar results have been reported for differentiating human EBs. Specifically, HAS-2 and its binding receptor, RHAMM, were highly upregulated in human EBs and preimplantation human embryos compared with ESCs, and a 24-fold enhancement of total hyaluronan was found in day 4 EBs (17.2 ng/10^6 cells) compared with ESCs (0.7 ng/10^6 cells) (Choudhary et al. 2007; Nairn et al. 2007). However, compared with both HAS-1 and HAS-3, increased expression of HAS-2 by human ESCs occurred only upon EB differentiation, whereas in the present study, HAS-2 expression was significantly greater than HAS-1 or HAS-3 in undifferentiated mESCs, as well as in EBs, at all time points examined. These subtle differences in HAS expression could be due to different culture methods utilized for the propagation and differentiation of mouse and human ESCs, as well as intrinsic differences between pluripotent cells derived from the two species (Tesar et al. 2007).

In addition to changes in HAS expression and hyaluronan synthesis, differentiating ESCs also exhibit temporal changes in versican isoform expression, associated with increasing versican content within EBs over the course of differentiation. In the developing embryo, versican plays an important role in early cell migration events during neural crest formation and cardiac morphogenesis (Henderson and Copp 1998; Dutt et al. 2006); thus, it is not surprising that versican is expressed by EBs undergoing similar differentiation processes in vitro. Compared with several other hyaluronan-binding proteoglycans, including aggrecan, neurocan, and brevican, previous work demonstrated that the transcript of versican was the only transcript to show a considerable enhancement in EBs compared with ESCs (Nairn et al. 2007). In the present study, however, gene expression of each of the four different versican isoforms was independently examined. Isoforms *V0* and *V1* were consistently expressed at greater levels than those of *V2* and *V3* throughout EB differentiation,

and by 10 days of differentiation, expression levels of *V0* and *V1* was significantly increased compared with that of earlier stages of differentiation. The V0 and V1 isoforms uniquely contain the β-GAG chain, and immunostaining and Western blotting results with an anti-β-GAG antibody clearly indicated accumulating versican (V0 and V1) protein within EBs after 7 days of differentiation. Specific expression of β-GAG isoforms (V0 and V1) has previously been linked to developmental processes such as chondrogenic differentiation and neural crest migration (Landolt et al. 1995; Perissinotto et al. 2000; Dutt et al. 2006; Kamiya et al. 2006), thus the V0 and V1 isoforms could be exerting similar effects on early ESC morphogenesis. Furthermore, proteolytic cleavage of versican by ADAMTS enzymes that expose the DPEAAE epitope (common to all four versican isoforms) has been associated with EMT during cardiac cushion formation in the mouse embryo (Kern et al. 2006) and has been reported to play an important signaling function in EMT processes in various tissues (Nakamura et al. 2005; Sone et al. 2005). In addition, expression of ADAMTS-5 was limited prior to 11.5 days (E11.5) of mouse embryogenesis but specifically found in developing nerves and limbs after E11.5, suggesting the potential importance of ADAMTS-5 in mid-stage development (McCulloch et al. 2009). Therefore, the coincidental increase in DPEAAE epitope exposure with the expression of ADAMTS-1 and ADAMTS-5 during EB differentiation indicates that similar remodeling processes are involved in pluripotent stem cell morphogenesis.

Differentiating ESCs offer a unique model for studying various aspects of developmental biology. Analyzing the dynamics of ECM synthesis, accumulation, and organization during development may yield new insights into the molecular regulatory mechanisms responsible for stimulating morphogenic processes, such as EMT, which is important for embryonic cell differentiation and organ development. In a broader context, these results also indicate that phenotypic differences between differentiating ESCs may be associated with the local composition of the ECM and, therefore, regulation of endogenous ECM production within EBs could provide a novel approach to directing ESC fate.

Acknowledgments

This research was funded by the Georgia Tech/Emory Center for the Engineering of Living Tissues (GTEC, National Science Foundation EEC-9731463), the National Institutes of Health (NIH) (R21 EB007316), and the American Heart Association (0665265B). R.N. is supported by a National Science Foundation fellowship. T.N.W. (R24 HL64387-06A1) and M.W.R. (F32 HL083593) were also supported by the NIH.

The authors thank Elizabeth Krauth at the Georgia Institute of Technology, Atlanta, GA, for technical assistance.

Literature Cited

Allison DD, Grande-Allen KJ (2006) Review. Hyaluronan: a powerful tissue engineering tool. Tissue Eng 12:2131–2140

Bain G, Kitchens D, Yao M, Huettner JE, Gottlieb DI (1995) Embryonic stem cells express neuronal properties in vitro. Dev Biol 168:342–357

Behr R, Heneweer C, Viebahn C, Denker HW, Thie M (2005) Epithelial-mesenchymal transition in colonies of rhesus monkey embryonic stem cells: a model for processes involved in gastrulation. Stem Cells 23:805–816

Camenisch TD, Spicer AP, Brehm-Gibson T, Biesterfeldt J, Augustine ML, Calabro A Jr, Kubalak S, et al. (2000) Disruption of hyaluronan synthase-2 abrogates normal cardiac morphogenesis and hyaluronan-mediated transformation of epithelium to mesenchyme. J Clin Invest 106:349–360

Carpenedo RL, Sargent CY, McDevitt TC (2007) Rotary suspension culture enhances the efficiency, yield, and homogeneity of embryoid body differentiation. Stem Cells 25:2224–2234

Choudhary M, Zhang X, Stojkovic P, Hyslop L, Anyfantis G, Herbert M, Murdoch AP, et al. (2007) Putative role of hyaluronan and its related genes, HAS2 and RHAMM, in human early preimplantation embryogenesis and embryonic stem cell characterization. Stem Cells 25:3045–3057

D'Amour KA, Agulnick AD, Eliazer S, Kelly OG, Kroon E, Baetge EE (2005) Efficient differentiation of human embryonic stem cells to definitive endoderm. Nat Biotechnol 23:1534–1541

D'Amour KA, Bang AG, Eliazer S, Kelly OG, Agulnick AD, Smart NG, Moorman MA, et al. (2006) Production of pancreatic hormone-expressing endocrine cells from human embryonic stem cells. Nat Biotechnol 24:1392–1401

Denker HW, Behr R, Heneweer C, Viebahn C, Thie M (2007) Epithelial-mesenchymal transition in Rhesus monkey embryonic stem cell colonies: a model for processes involved in gastrulation? Cells Tissues Organs 185:48–50

Doetschman TC, Eistetter H, Katz M, Schmidt W, Kemler R (1985) The in vitro development of blastocyst-derived embryonic stem cell lines: formation of visceral yolk sac, blood islands and myocardium. J Embryol Exp Morphol 87:27–45

Dutt S, Kleber M, Matasci M, Sommer L, Zimmermann DR (2006) Versican V0 and V1 guide migratory neural crest cells. J Biol Chem 281:12123–12131

Eastham AM, Spencer H, Soncin F, Ritson S, Merry CL, Stern PL, Ward CM (2007) Epithelial-mesenchymal transition events during human embryonic stem cell differentiation. Cancer Res 67:11254–11262

Evans MJ, Kaufman MH (1981) Establishment in culture of pluripotential cells from mouse embryos. Nature 292:154–156

Fenderson BA, Stamenkovic I, Aruffo A (1993) Localization of hyaluronan in mouse embryos during implantation, gastrulation and organogenesis. Differentiation 54:85–98

Ffrench-Constant C, Hynes RO (1989) Alternative splicing of fibronectin is temporally and spatially regulated in the chicken embryo. Development 106:375–388

Foschi D, Castoldi L, Radaelli E, Abelli P, Calderini G, Rastrelli A, Mariscotti C, et al. (1990) Hyaluronic acid prevents oxygen free-radical damage to granulation tissue: a study in rats. Int J Tissue React 12:333–339

Gossler A, Joyner AL, Rossant J, Skarnes WC (1989) Mouse embryonic stem cells and reporter constructs to detect developmentally regulated genes. Science 244:463–465

Henderson DJ, Copp AJ (1998) Versican expression is associated with chamber specification, septation, and valvulogenesis in the developing mouse heart. Circ Res 83:523–532

Itskovitz-Eldor J, Schuldiner M, Karsenti D, Eden A, Yanuka O, Amit M, Soreq H, et al. (2000) Differentiation of human embryonic stem cells into embryoid bodies compromising the three embryonic germ layers. Mol Med 6:88–95

Kamiya N, Watanabe H, Habuchi H, Takagi H, Shinomura T, Shimizu K, Kimata K (2006) Versican/PG-M regulates chondrogenesis as an extracellular matrix molecule crucial for mesenchymal condensation. J Biol Chem 281:2390–2400

Kenagy RD, Plaas AH, Wight TN (2006) Versican degradation and vascular disease. Trends Cardiovasc Med 16:209–215

Kern CB, Twal WO, Mjaatvedt CH, Fairey SE, Toole BP, Iruela-Arispe ML, Argraves WS (2006) Proteolytic cleavage of versican during cardiac cushion morphogenesis. Dev Dyn 235:2238–2247

Kishimoto J, Ehama R, Wu L, Jiang S, Jiang N, Burgeson RE (1999) Selective activation of the versican promoter by epithelial-mesenchymal interactions during hair follicle development. Proc Natl Acad Sci USA 96:7336–7341

Landolt RM, Vaughan L, Winterhalter KH, Zimmermann DR (1995) Versican is selectively expressed in embryonic tissues that act as barriers to neural crest cell migration and axon outgrowth. Development 121:2303–2312

Longpre JM, McCulloch DR, Koo BH, Alexander JP, Apte SS, Leduc R (2009) Characterization of proADAMTS5 processing by proprotein convertases. Int J Biochem Cell Biol 41:1116–1126

Martin GR (1981) Isolation of a pluripotent cell line from early mouse embryos cultured in medium conditioned by teratocarcinoma stem cells. Proc Natl Acad Sci USA 78:7634–7638

McCulloch DR, Goff CL, Bhatt S, Dixon LJ, Sandy JD, Apte SS (2009) Adamts5, the gene encoding a proteoglycan-degrading metalloprotease, is expressed by specific cell lineages during mouse embryonic development and in adult tissues. Gene Expr Patterns 9:314–323

Mjaatvedt CH, Yamamura H, Capehart AA, Turner D, Markwald RR (1998) The Cspg2 gene, disrupted in the hdf mutant, is required for right cardiac chamber and endocardial cushion formation. Dev Biol 202:56–66

Nairn AV, Kinoshita-Toyoda A, Toyoda H, Xie J, Harris K, Dalton S, Kulik M, et al. (2007) Glycomics of proteoglycan biosynthesis in murine embryonic stem cell differentiation. J Proteome Res 6:4374–4387

Nakamura M, Sone S, Takahashi I, Mizoguchi I, Echigo S, Sasano Y (2005) Expression of versican and ADAMTS1, 4, and 5 during bone development in the rat mandible and hind limb. J Histochem Cytochem 53:1553–1562

Perissinotto D, Iacopetti P, Bellina I, Doliana R, Colombatti A, Pettway Z, Bronner-Fraser M, et al. (2000) Avian neural crest cell migration is diversely regulated by the two major hyaluronan-binding proteoglycans PG-M/versican and aggrecan. Development 127:2823–2842

Pfaffl MW (2001) A new mathematical model for relative quantification in real-time RT-PCR. Nucleic Acids Res 29:e45

Ricciardelli C, Russell DL, Ween MP, Mayne K, Suwiwat S, Byers S, Marshall VR, et al. (2007) Formation of hyaluronan- and versican-rich pericellular matrix by prostate cancer cells promotes cell motility. J Biol Chem 282:10814–10825

Robbins J, Gulick J, Sanchez A, Howles P, Doetschman T (1990) Mouse embryonic stem cells express the cardiac myosin heavy chain genes during development in vitro. J Biol Chem 265:11905–11909

Sandy JD, Westling J, Kenagy RD, Iruela-Arispe ML, Verscharen C, Rodriguez-Mazaneque JC, Zimmermann DR, et al. (2001) Versican V1 proteolysis in human aorta in vivo occurs at the Glu441-Ala442 bond, a site that is cleaved by recombinant ADAMTS-1 and ADAMTS-4. J Biol Chem 276:13372–13378

Schoenfelder M, Einspanier R (2003) Expression of hyaluronan synthases and corresponding hyaluronan receptors is differentially regulated during oocyte maturation in cattle. Biol Reprod 69:269–277

Seidelmann SB, Kuo C, Pleskac N, Molina J, Sayers S, Li R, Zhou J, et al. (2008) Athsq1 is an atherosclerosis modifier locus with dramatic effects on lesion area and prominent accumulation of versican. Arterioscler Thromb Vasc Biol 28:2180–2186

Sone S, Nakamura M, Maruya Y, Takahashi I, Mizoguchi I, Mayanagi H, Sasano Y (2005) Expression of versican and ADAMTS during rat tooth eruption. J Mol Histol 36:281–288

Spencer HL, Eastham AM, Merry CL, Southgate TD, Perez-Campo F, Soncin F, Ritson S, et al. (2007) E-cadherin inhibits cell surface localization of the pro-migratory 5T4 oncofetal antigen in mouse embryonic stem cells. Mol Biol Cell 18:2838–2851

Spicer AP, Tien JL, Joo A, Bowling RA Jr (2002) Investigation of hyaluronan function in the mouse through targeted mutagenesis. Glycoconj J 19:341–345

Tesar PJ, Chenoweth JG, Brook FA, Davies TJ, Evans EP, Mack DL, Gardner RL, et al. (2007) New cell lines from mouse epiblast share defining features with human embryonic stem cells. Nature 448:196–199

Thomson JA, Itskovitz-Eldor J, Shapiro SS, Waknitz MA, Swiergiel JJ, Marshall VS, Jones JM (1998) Embryonic stem cell lines derived from human blastocysts. Science 282:1145–1147

Toole BP (2004) Hyaluronan: from extracellular glue to pericellular cue. Nat Rev Cancer 4:528–539

Toole BP, Zoltan-Jones A, Misra S, Ghatak S (2005) Hyaluronan: a critical component of epithelial-mesenchymal and epithelial-carcinoma transitions. Cells Tissues Organs 179:66–72

Trabucchi E, Pallotta S, Morini M, Corsi F, Franceschini R, Casiraghi A, Pravettoni A, et al. (2002) Low molecular weight hyaluronic acid prevents oxygen free radical damage to granulation tissue during wound healing. Int J Tissue React 24:65–71

Ullmann U, In't Veld P, Gilles C, Sermon K, De Rycke M, Van de Velde H, Van Steirteghem A, et al. (2007) Epithelial-mesenchymal transition process in human embryonic stem cells cultured in feeder-free conditions. Mol Hum Reprod 13:21–32

Wan YJ, Wu TC, Chung AE, Damjanov I (1984) Monoclonal antibodies to laminin reveal the heterogeneity of basement membranes in the developing and adult mouse tissues. J Cell Biol 98:971–979

West DC, Hampson IN, Arnold F, Kumar S (1985) Angiogenesis induced by degradation products of hyaluronic acid. Science 228:1324–1326

Wight TN (2002) Versican: a versatile extracellular matrix proteoglycan in cell biology. Curr Opin Cell Biol 14:617–623

Wight TN, Merrilees MJ (2004) Proteoglycans in atherosclerosis and restenosis: key roles for versican. Circ Res 94:1158–1167

Wobus AM, Holzhausen H, Jakel P, Schoneich J (1984) Characterization of a pluripotent stem cell line derived from a mouse embryo. Exp Cell Res 152:212–219

Zoltan-Jones A, Huang L, Ghatak S, Toole BP (2003) Elevated hyaluronan production induces mesenchymal and transformed properties in epithelial cells. J Biol Chem 278:45801–45810

The Journal of Histochemistry & Cytochemistry